PAPER • **OPEN ACCESS**

Deceleration of the Cold Flow in the Vortex Tube

To cite this article: N Anoshin *et al* 2020 *IOP Conf. Ser.: Mater. Sci. Eng.* **972** 012077

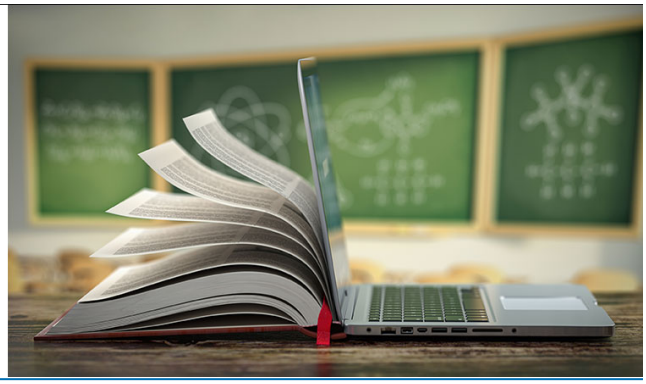

IOP Conf. Series: Materials Science and Engineering **972** (2020) 012077 doi:10.1088/1757-899X/972/1/012077

Deceleration of the Cold Flow in the Vortex Tube

N Anoshin[1], A Khait[1], V Bianco[2], A Noskov[1], V Alekhin[1]

[1]Ural Federal University, 19 Mira St., 620002 Ekaterinburg, Russia

[2] DIME/TEC – Division of Thermal Energy and Environmental Conditioning, University of Genoa, Via All'Opera Pia 15A, 16145 Genoa, Italy

E-mail: n.m.anoshin@urfu.ru

Abstract. Enhancement of the cold flow deceleration unit is considered in the paper to improve the energetic efficiency of the vortex tube. It was shown that the gradual expansion of the cross-section in the cold flow diffuser is inefficient for reducing the gas flow velocity in presence of its significant rotation. Installation of a blade grid at the entrance to the cold flow diffuser was suggested for interruption of the flow swirling. A notable reduction of the energy losses has been demonstrated improving the efficiency of the vortex tube.

Keywords: vortex tube, efficiency, deceleration

1. Introduction

The effect of temperature stratification in the vortex flows known also as a Ranque-Hilsch effect is thoroughly investigated both theoretically and experimentally. However, the reasons for the appearance of such a phenomenon are still not well understood [1, 2]. The main difficulty here is the requirement for the velocities of the gas to be extremely high (nearly trans-sonic) to distinguish the effect. The resultant flow appears to be strongly turbulent that significantly complicates any theoretical considerations.

Nevertheless, the Ranque-Hilsch effect has found its application in the devices called vortex tubes that are widely utilized for cooling or heating the pressurized gas. The lack in the complete theoretical understanding of the physical processes involved in the operation of the vortex tubes stipulates a relatively low efficiency of such devices. One of the available ways to improve the performance of the vortex tube is the optimization of its design by performing the numerical or physical experiments.

Following this approach, the influence of the divergence angle of the energy separation chamber was investigated experimentally in [3]. It was shown that the optimal value of the angle lays within the range 2-4°. The number of the inlet nozzle channels and their convergence ratio, length of the energy separation chamber, cold orifice diameter and inlet pressure were studied in [3, 4] and optimized experimentally in [5]. The method of the local entropy generation analysis was implemented in [6] to find the ways for further optimization of the vortex tube performance.

Efficient deceleration of the gas flow before its release from the vortex tube to the ambient environment constitutes also a significant problem. In view of this, the effect of the angle of the hot control valve on the vortex tube efficiency was considered in [7]. On the other hand, the influence of the shape of this valve has been studied in [8]. The spiral motion of the gas at very high velocities

makes the deceleration of the flow at the cold outlet of the vortex tube to be a significantly more complicated task. The diffusers having different orifice diameter and divergence angle were tested in [9]. A notable influence of the diffuser angle on the vortex tube efficiency was reported. This points to the insufficient efficiency of the classical design of the cold outlet of the vortex tube. Fins of different shapes were introduced to the geometry of the cold flow diffuser in [10] attempting to reduce the energy losses.

It should be highlighted that in all previous studies the rotation of the gas flow at the cold outlet of the vortex tube has not been taken into account. In this paper we devote a particular attention to interruption of the rotation of the gas flow before its output from the vortex tube. This is expected to allow the reduction of the energy losses associated with the subsequent deceleration process in the cold flow diffuser. Interruption of the gas flow rotation is performed by the specifically designed blade grids having different configurations. The reduction of the energy losses in the cold flow deceleration process will potentially influence the increase of the vortex tube efficiency.

2. Vortex Tube and the cold flow deceleration unit

The domain of the vortex tube is shown in Fig. 1. Pressurized air is supplied to the nozzle inlet 1 consisting of six curved rectangular channels. Reduction of the cross-section of each channel leads to the acceleration of the air to the velocities close to the speed of sound. Accelerated air is then passed to the energy separation chamber 2 having a conical shape. Radial temperature stratification arises in the vortex flow generated in the chamber 2 such that the core region of the vortex has lower total (stagnation) temperature compared to the outer region. The heated air is let out via the left side of the vortex tube, see Fig. 1, whereas the cooled air from the vortex core is exhausted via the opposite side.

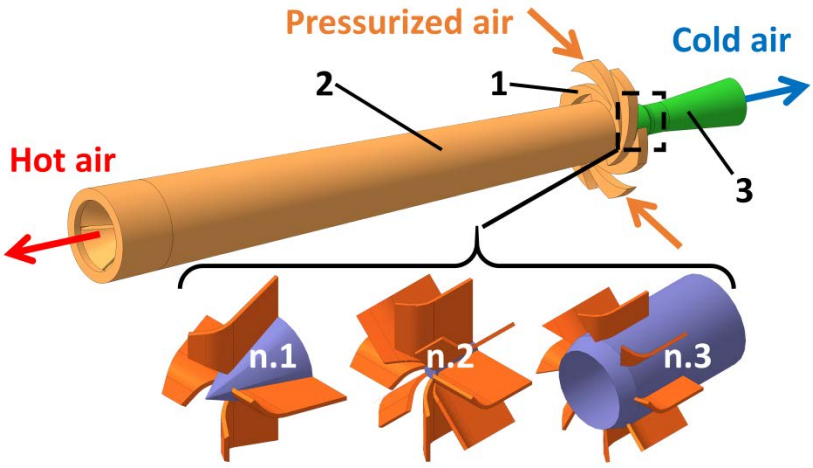

Fig. 1. Schematic of the vortex tube with different blade grids at the cold flow outlet: 1 - nozzle inlet to the vortex tube; 2 - energy separation chamber; 3 - cold flow diffuser

Deceleration of the cold air before its release from the vortex tube to the ambient environment is presently performed by the diffuser 3 (Fig. 1). The reduction of the cold air velocity within the diffuser is expected due to the increase of the cross-section area. Such configuration was proved to be efficient for the unidirectional coaxial flows. Because of the existence of a significant rotational component in the cold flow, application of the simple diffuser is inefficient for the vortex tubes. In this study we attempt to increase the efficiency of the cold flow deceleration by improvement of the configuration of the diffuser 3 (Fig. 1). The suggested method of the vortex flow deceleration consists of two stages. First, we interrupt the rotation of the flow while passing through the blade grids. This will allow to obtain a coaxial flow that may be decelerated in the diffuser.

Different configurations of the blade grids denoted as n.1 – n.3 were considered, see Fig. 1. It is known that the radial distribution of the rotational component of the velocity in the flow under consideration is linear with a negligibly small rotation in the center. Thus, in the first case (n.1), we place the blades only at the outer part of the diffuser and fill the center by the conical body. Second configuration (n.2) incorporates the blades that occupy the entire cross-section. The last option (n.3) is

similar to n.1 except for the shape of the body placed in the center. Now we utilize a short tube allowing the core part of the flow to pass the deceleration unit while maintaining the rotation.

3. Numerical model

Numerical model of 3D flow of compressible viscous air was utilized to test the performance of different configurations of the vortex tube shown in Fig. 1. Since the flow under consideration is strongly turbulent, the model was based on Reynolds-Averaged Navier-Stokes (RANS) equations closed with the standard k-ε turbulence model. Ideal gas state equation was used to take into account the dependence of the air density on its static pressure and temperature. The conservation of the energy of the system was ensured by solving the equation for the total enthalpy, which in the case of the ideal gas is $H = c_p T + V^2/2$. The properties of the air were defined by the following constants: gas constant R = 287 $J/(kg\ K)$; dynamic viscosity $\mu = 1.831\times10^{-5}$ $Pa\ s$; thermal conductivity λ = 0.0261 $J/(m\ s\ K)$; heat capacity c_p = 1004.4 $J/(kg\ K)$. The constants of the k-ε turbulence model were selected as follows: $C_{\varepsilon 1}$ = 1.44; $C_{\varepsilon 2}$ = 1.92; C_μ = 0.09; σ_k = 1.0; σ_ε = 1.3.

The ANSYS CFX software was used for the numerical solution of the equations using the Finite-Volume Method. High resolution advection scheme was used for estimation of the spatial derivatives, while second-order implicit scheme was used for the temporal integration. Adaptive time step within $\Delta t = 10^{-5}$ - 10^{-7} s was applied. The structured hexahedral mesh consisting of 430 000 cells was utilized to approximate the geometry of the nozzle inlet and the energy separation chamber. On the other hand, the geometry of the cold flow deceleration unit incorporating the blade grid was described by the unstructured tetrahedral mesh consisting of 140 000 – 160 000 cells depending on the particular configuration n.1 – n.3, see Fig. 1. We refer to [6] for the better details on the numerical model.

The dimensions of the domain and the operational parameters of the vortex tube are summarized in Table 1. Operation regime of the vortex tube is usually characterized by the value of the so-called cold flow fraction given as

$$\varphi = G_c / G_i \,, \tag{1}$$

where G_c and G_i are the mass flow rates of the cold and the inlet flows respectively. In turn, the efficiency of the vortex tube is estimated by the following coefficient:

$$\eta = \varphi \frac{T_i^* - T_c^*}{T_i^* \left[1 - \left(\frac{p_c^*}{p_i^*} \right)^{\frac{\gamma-1}{\gamma}} \right]} \tag{2}$$

Here superscript * denotes the stagnation value of the quantity; γ = 1.4 is the adiabatic index.

4. Results and discussion

First, we study the flow observed in the base configuration of the deceleration unit corresponding to the standard conical diffuser without the blades installed. The velocity field in the longitudinal section of such diffuser is shown in Fig. 2(a). It is seen that the velocity magnitudes reach quite significant values around 250 m/s. Because of the centrifugal force caused by the strong rotation of the air, gradual increase of the diameter of the diffuser leads to the reduction of the pressure in the core part where the rotation is almost absent. In the considered case, the pressure drops even below the ambient value leading to the appearance of the large-scale secondary circulation clearly seen in Fig. 2(a). Existence of such a circulation is considered to be one of the main reason of the low efficiency of the deceleration unit.

As seen from Fig. 2(b), deceleration unit n.1 redistributes the velocity in the cross-sections such that the high speed area is now concentrated near the outer walls, whereas the velocity value in the core region is notably reduced. Such a flow configuration shortens the large-scale secondary

circulation. Implementation of the deceleration unit n.2, see Fig. 2(c), gives even smoother flow with almost constant value of the velocity in every cross-section of the diffuser. The rotational component of the velocity is effectively cancelled, and the secondary circulation is fully suppressed in this case.

Table 1. Dimensions and operation parameters of the vortex tube

	Value	Units
Diameter of the energy separation chamber	16	mm
Length of the energy separation chamber	170	mm
Diameter of the diaphragm	9.5	mm
Cone angle	2	°
Gauge pressure of the supplied air, p_{in}^*	300	kPa
Stagnation temperature of the supplied air, T_{in}^*	300	K
Cold flow fraction	0.1 – 0.8	-

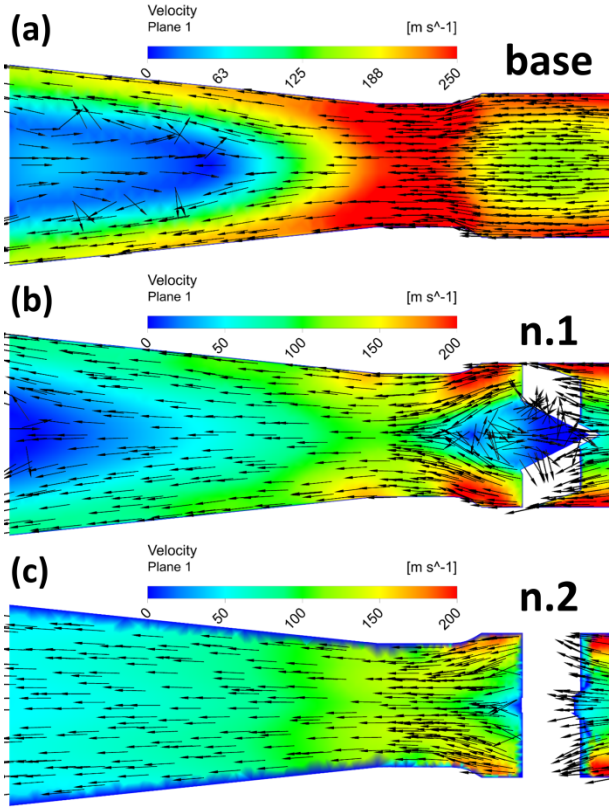

Fig. 2. Distribution of the velocity magnitude [m/s] over the longitudinal section of the cold flow diffuser: (a) base configuration without blades; (b) deceleration unit n.1; (c) deceleration unit n.2

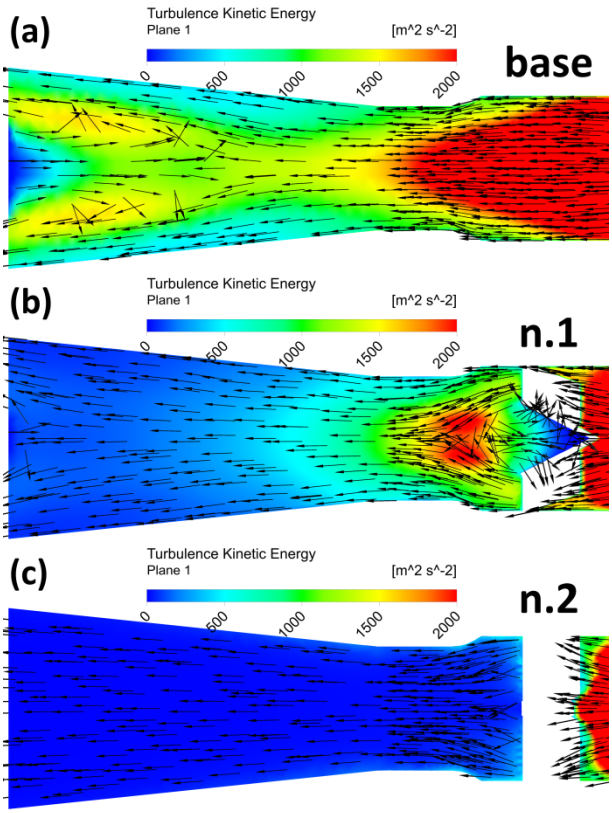

Fig. 3. As in Fig. 2 for the turbulence kinetic energy [m^2/s^2]

In Fig. 3 we study the distribution of the turbulence energy in the longitudinal section of different deceleration units. It is notable that the base configuration shows the strongest turbulization of the flow. In the unit n.1, the turbulence is concentrated only in the proximity of the blade grid, while the turbulence in the unit n.2 is very low in all cross-sections after the blades, cf. Figs. 3(b) and (c).

Taking into account that the irreversible energy losses in *k-ε* turbulence model are proportional to the square of the turbulence kinetic energy, the utilization of the deceleration unit n.2 is expected to improve the efficiency of the vortex tube as compared to the base design.

Despite the low values of the rotational velocity in the center of the cold flow deceleration unit, application of the blade grid n.3 gave rise to the flow instability. An extremely unstable secondary vortex structure originated from the central flow is observed in Fig. 4. Increase of the turbulence in this case is expected to provoke the additional energy losses and, consequently, the reduction of the efficiency.

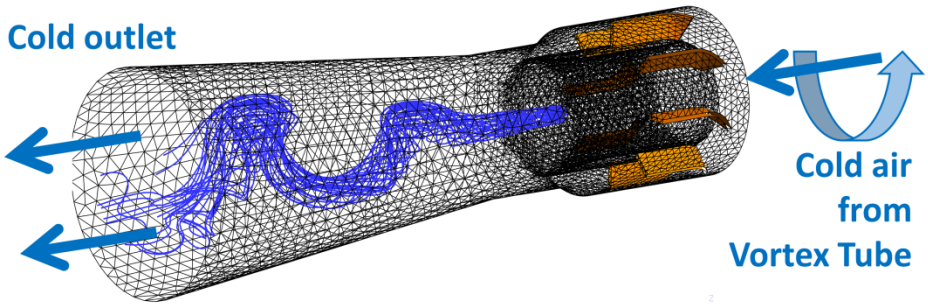

Fig. 4. Secondary vortex structure observed in the deceleration unit n.3

The main energetic characteristic of the vortex tube is plotted in Fig. 5 as function $\eta = \eta(\varphi)$. The highest value of the energy efficiency coefficient (2) is found at the cold flow fraction (1) $\varphi \approx 0.6$ in agreement with the previous investigations. As expected, installation of the deceleration unit n.3 reduced the efficiency as compared to the base design of the vortex tube. On the other hand, unit n.2 (see Fig. 1) allowed a notable improvement of the vortex tube performance. Taking into account that the design of the unit n.2 is not optimal, the efficiency may be increased even further after the corresponding optimization.

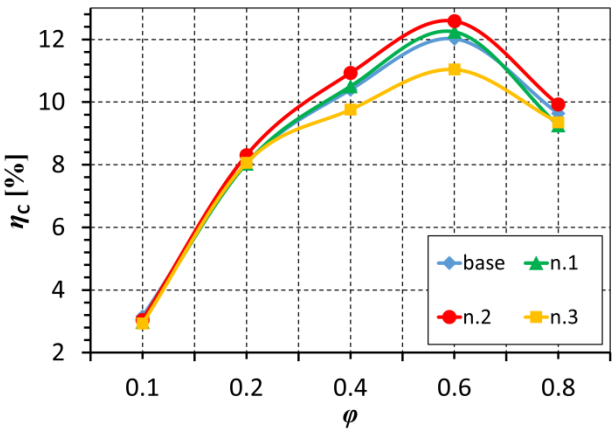

Fig. 5. Energy efficiency of the vortex tube (2) as a function of the cold flow fraction (1)

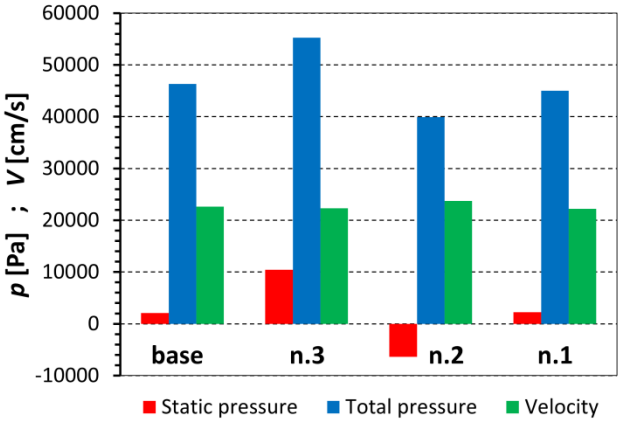

Fig. 6. Mass-flow averaged values of the gauge pressure and the velocity at the entrance to the deceleration units

A physical insight on the reasons of the efficiency improvement may be found from the analysis of the integral value of the mass-flow averaged static gauge pressure at the entrance to the deceleration unit. Fig. 6 shows that the velocity magnitudes at the entrance to the deceleration units are similar in all the considered designs. On the other hand, there is an obvious trend showing that the lower static pressure is observed at the entrance to the deceleration unit the higher efficiency of the vortex tube is obtained. In case the unit n.2 is applied, the static gauge pressure drops even below the ambient value.

Reduction of the given pressure causes increase of the available pressure difference (pressure ratio) between the inlet to the vortex tube and the outlet from the energy separation chamber (2 in Fig. 1).

5. Conclusion

In this study we attempted to reduce the energy losses involved in the deceleration of the gas flow at the cold outlet of the vortex tube. For that purpose, different blade grids were placed before the inlet to the cold flow diffuser. The blades were designed to interrupt the rotation of the air flow. Once the rotation is cancelled, the velocity of the air is efficiently reduced by expanding the cross-section in the diffuser.

It was found that the installation of the blade grids may result in reduction of the flow turbulization. Straightening of the flow allowed avoiding appearance of the secondary recirculation at the cold outlet and notably increased the efficiency of the vortex tube. The physical justification of the improvement of the vortex tube efficiency was found in the analysis of the mass-flow averaged values of the static pressure at the entrance to the deceleration unit. Reduction of this pressure provoked the increase of the available pressure ratio and, consequently, the available work.

It should be emphasized that the geometry of the deceleration units examined in the present paper cannot be considered as optimal. Therefore, the optimization of several constructive parameters of the blade grids and the diffuser may theoretically lead to even more significant increase of the vortex tube efficiency.

References

[1] J. Lagrandeur, S. Poncet, M. Sorin 2019 Review of predictive models for the design of counterflow vortex tubes working with perfect gas *Int. J. Therm. Sci*. **142** 188–204
[2] A. Khait, A. Noskov, A. Lovtsov, V. Alekhin 2014 Semi-empirical turbulence model for numerical simulation of swirled compressible flows observed in Ranque-Hilsch vortex tube *Int. J. Refrig* **48** 132-141
[3] K. Chang, Q. Li, G. Zhou, Q. Li 2011 Experimental investigation of vortex tube refrigerator with a divergent hot tube *Int. J. Refrig*. **34** 322–327
[4] S.E. Rafiee, M. Rahimi 2013 Experimental study and three-dimensional (3D) computational fluid dynamics (CFD) analysis on the effect of the convergence ratio, pressure inlet and number of nozzle intake on vortex tube performance - Validation and CFD optimization *Energy* **63** 195–204
[5] M. Bovand, M.S. Valipour, K. Dincer, S. Eiamsa-Ard 2014 Application of response surface methodology to optimization of a standard Ranque-Hilsch vortex tube refrigerator *Appl. Therm. Eng*. **67** 545–553
[6] A. Khait, A. Noskov, V. Alekhin, V. Bianco 2018 Analysis of the local entropy generation in a double-circuit vortex tube *Appl. Therm. Eng.* **130** 1391–1403
[7] K. Dincer, S. Baskaya, B.Z. Uysal, I. Ucgul 2009 Experimental investigation of the performance of a Ranque-Hilsch vortex tube with regard to a plug located at the hot outlet, *Int. J. Refrig.* **32** 87–94
[8] S.E. Rafiee, M.M. Sadeghiazad 2017 Experimental and 3D CFD investigation on heat transfer and energy separation inside a counter flow vortex tube using different shapes of hot control valves *Appl. Therm. Eng.* **110** 648–664
[9] M. Farzaneh-Gord, M. Sadi 2014 Improving vortex tube performance based on vortex generator design *Energy* **72** 492–500
[10] A. Bazgir, A. Heydari, N. Nabhani 2019 Investigation of the thermal separation in a counter-flow Ranque-Hilsch vortex tube with regard to different fin geometries located inside the cold-tube length, *Int. Commun. Heat Mass* **108** 104273